

Presence of an oligodendroglioma-like component in newly diagnosed glioblastoma identifies a pathogenetically heterogeneous subgroup and lacks prognostic value: central pathology review of the EORTC_26981/NCIC_CE.3 trial

Monika E. Hegi · Robert-Charles Janzer · Wanyu L. Lambiv · Thierry Gorlia · Mathilde C. M. Kouwenhoven · Christian Hartmann · Andreas von Deimling · Danielle Martinet · Nathalie Besuchet Schmutz · Annie-Claire Diserens · Marie-France Hamou · Pierre Bady · Michael Weller · Martin J. van den Bent · Warren P. Mason · René-Olivier Mirimanoff · Roger Stupp · Karima Mokhtari · Pieter Wesseling

Received: 4 December 2011 / Revised: 29 December 2011 / Accepted: 30 December 2011 / Published online: 15 January 2012
© Springer-Verlag 2012

Abstract Glioblastoma (GBM) is a morphologically heterogeneous tumor type with a median survival of only 15 months in clinical trial populations. However, survival varies greatly among patients. As part of a central pathology review, we addressed the question if patients with GBM displaying distinct morphologic features respond

differently to combined chemo-radiotherapy with temozolomide. Morphologic features were systematically recorded for 360 cases with particular focus on the presence of an oligodendroglioma-like component and respective correlations with outcome and relevant molecular markers. GBM with an oligodendroglioma-like component (GBM-O) represented 15% of all confirmed GBM (52/339) and was not associated with a more favorable outcome. GBM-O encompassed a pathogenetically heterogeneous group, significantly enriched for *IDH1* mutations (19 vs. 3%, $p = 0.003$) and *EGFR* amplifications (71 vs. 48%, $p = 0.04$) compared with other GBM, while co-deletion of 1p/19q was found in only one case and the *MGMT* methylation frequency was alike (47 vs. 46%). Expression profiles classified most of the GBM-O into two subtypes, 36% (5/14 evaluable) as proneural and 43% as

This work is dedicated to the memory of the late Dr. Robert-Charles Janzer who suddenly died in 2010. RCJ outlined the morphological analysis and coordinated central pathology review of this study.

On behalf of the European Organisation for Research and Treatment of Cancer Brain Tumour and Radiation Oncology Groups and the National Cancer Institute of Canada Clinical Trials Group.

Electronic supplementary material The online version of this article (doi:10.1007/s00401-011-0938-4) contains supplementary material, which is available to authorized users.

M. E. Hegi · W. L. Lambiv · A.-C. Diserens · M.-F. Hamou · P. Bady · R. Stupp
Department of Clinical Neurosciences, Lausanne University Hospital, Lausanne, Switzerland

M. E. Hegi
National Center of Competence in Research Molecular Oncology, ISREC-SV-EPFL, Lausanne, Switzerland

R.-C. Janzer
Department of Pathology, Lausanne University Hospital, Lausanne, Switzerland

T. Gorlia
European Organisation for Research and Treatment of Cancer (EORTC) Headquarters, Brussels, Belgium

M. C. M. Kouwenhoven · M. J. van den Bent
Department of Neurology, Erasmus Medical Center, Rotterdam, The Netherlands

C. Hartmann · A. von Deimling
Department of Neuropathology, Institute of Pathology, Ruprecht-Karls-University, Heidelberg, Germany

C. Hartmann · A. von Deimling
Clinical Cooperation Unit Neuropathology, DKFZ, Heidelberg, Germany

D. Martinet · N. Besuchet Schmutz
Department of Medical Genetics, Lausanne University Hospital, Lausanne, Switzerland

P. Bady
Bioinformatics Core Facility, Swiss Institute for Bioinformatics, Lausanne, Switzerland

M. Weller
Department of Neurology, University of Tübingen, Tübingen, Germany

classical GBM. The detection of pseudo-palisading necrosis (PPN) was associated with benefit from chemotherapy ($p = 0.0002$), while no such effect was present in the absence of PPN ($p = 0.86$). In the adjusted interaction model including clinical prognostic factors and *MGMT* status, PPN was borderline nonsignificant ($p = 0.063$). Taken together, recognition of an oligodendroglioma-like component in an otherwise classic GBM identifies a pathogenetically mixed group without prognostic significance. However, the presence of PPN may indicate biological features of clinical relevance for further improvement of therapy.

Keywords Glioblastoma · Glioblastoma with oligodendroglioma-like component · *MGMT* · *IDH1* · *EGFR* · Pathology · Temozolomide · Randomized trial · Pseudopalisading necrosis · Prognostic factors

Introduction

The introduction of combined chemo-radiotherapy adding temozolomide concomitantly and adjuvant to radiotherapy has modestly increased outcome of patients with newly diagnosed glioblastoma (GBM) [32], in particular in patients whose tumors contain an epigenetically inactivated *MGMT* gene [11]. However, outcome varies dramatically even in a homogeneously treated patient population with a median survival of 15 months: 2- and 5-year survival rates of 27 and 11%, respectively [7, 19, 21, 32]. Histopathologically, GBM is a heterogeneous tumor type and distinct morphologic subtypes may benefit differently from combined chemo-radiotherapy. Furthermore, unequivocal separation of GBM and anaplastic astrocytomas from anaplastic oligo-astrocytic neoplasms is difficult. Previous reports suggested that distinct morphologic features present in GBM may have prognostic value, such as the presence of an oligodendroglioma-like component that was

associated with better outcome in some studies, while the presence of necrosis has been reported as a negative prognostic factor [9, 12, 16, 18, 37].

Here, we addressed the question whether particular morphologic features in GBM can identify clinically meaningful subgroups in this patient cohort treated homogeneously with combined radio-chemotherapy that has become the standard of care. A specific goal was to investigate the clinical relevance of recognition of an oligodendroglioma-like component in GBM in tumors that had been diagnosed as GBM (all subtypes) by the initial local pathology assessment. The histopathological study was carried out as part of the central review performed in the phase III EORTC_26981-22981-NCIC_CE.3 trial for newly diagnosed GBM [32, 33]. The results of this detailed histopathological review were correlated with outcome and benefit from the new concomitant chemo-radiotherapy and in a subset of cases associated with genetic information including the *MGMT* methylation status, copy number aberrations (CNAs) of *EGFR*, *CDK4* and *MDM2*, combined loss of chromosomes 1p and 19q, and mutations of *IDH1*.

Patients and methods

Patients

Patients were enrolled in the phase III EORTC_26981-22981-NCIC_CE.3 trial [33] (ClinicalTrials.gov, number NCT00006353) between August 2000 and March 2002. Eligibility criteria have been detailed elsewhere [32] and comprised age between 18 and 70 years, histologically proven newly diagnosed GBM (WHO grade IV) and a WHO performance status of 0–2. Patients were randomized to either standard focal radiotherapy (RT) with a total dose of 60 Gy or concomitant chemotherapy of oral temozolomide (TMZ) at a daily dose of 75 mg/m² given 7 days per week during radiotherapy, followed by up to six cycles of

M. Weller
Department of Neurology, University Hospital Zurich,
Zurich, Switzerland

W. P. Mason
Princess Margaret Hospital, University of Toronto,
Toronto, Canada

R.-O. Mirimanoff
Department of Radio-Oncology,
Lausanne University Hospital, Lausanne, Switzerland

K. Mokhtari
Laboratoire de Neuropathologie R. Escourolle,
Groupe Hospitalier Pitié-Salpêtrière, Paris, France

P. Wesseling
Department of Pathology, Radboud University Nijmegen
Medical Centre, Nijmegen, The Netherlands

P. Wesseling
Department of Pathology, VU University Medical Center,
Amsterdam, The Netherlands

M. E. Hegi (✉)
Laboratory of Brain Tumor Biology and Genetics, Neurosurgery,
Centre Hospitalier Universitaire Vaudois (CHUV BH19-110),
46 rue du Bugnon, 1011 Lausanne, Switzerland
e-mail: Monika.Hegi@chuv.ch

adjuvant TMZ (150–200 mg/m²) for 5 days every 28 days. All patients had given written informed consent prior to entering the study, including for molecular analysis of their tumors. The study was approved by the local ethics committees.

Pathology review

Central review was performed jointly by three experienced neuropathologists (RCJ, KM, PW) according to WHO 2000 criteria [15] using a multiheaded microscope. H&E-stained full sections were used for the evaluation. In most cases GFAP-, MIB-1 and a reticulin silver stain were available (collectively performed in Lausanne). Morphologic features were systematically recorded in a semi-quantitative manner and comprised cellular differentiation patterns, types of necrosis (large ischemic type vs. pseudopalisading necrosis), microvascular proliferation and MIB-1 labeling index (see evaluation form, Supplementary Figure S1). In line with the WHO classification, pseudopalisading necrosis (PPN) was defined as irregular, often serpiginous foci of necrosis surrounded by densely packed, radially oriented tumor cells. The agreement between the three pathologists was recorded. For this study, GBM with an oligodendroglioma-like component (GBM-O) was defined according to the following histopathological criteria: presence of at least one of two “major criteria”—‘diffuse highly cellular and monotonous growth at low power magnification’, ‘monomorphous cell population’; and at least two of three “minor criteria”—‘perinuclear halo formation in tumor cells’, ‘rounded tumor cell nuclei with dense chromatin pattern’, ‘chickenwire architecture of tumor microvasculature’. The extent of these features in the viable tumor tissue was recorded (<25, 25–75, >75%). GBM with >25% of the tumor tissue showing

oligodendroglioma-like component was subclassified as GBM-O (see Fig. 1 for some examples).

Tissue microarray, immunohistochemistry and molecular analysis

Immunohistochemistry for GFAP and MIB-1, and histochemical reticulin staining were performed according to standard procedures on whole sections. A tissue microarray (TMA) was constructed comprising 130 patient samples where tumor blocks with sufficient tissue were available as reported previously [21]. The TMA was used to screen for the most common IDH1 mutation (R132H) using the specific antibody mIDH1R132H (clone H14) [4] and for copy number aberrations (CNAs) of selected genes by FISH. FISH for *EGFR* was performed as described [34]. Two-color FISH assay was performed using a mixed 1p36/1q25 and 19p13/19q13 dual color probe set (Cat. No 32-231004, Vysis, Inc., Applied Biosystems, Downers Grove, IL, USA) as described [31]. Samples showing sufficient FISH efficiency (~90% nuclei with signals) were evaluated. If possible, signals were scored in at least 200 non-overlapping, intact nuclei. Deletions of 1p and 19q were scored when at least 50% of tumor nuclei contained one signal. The following probes were used for *CDK4* and *MDM2*: KBI-10725 CD4K/SE12 (12q14); KBI-10717 MDM2/SE12 (12q15) (Kreatech Diagnostics, Amsterdam; The Netherlands).

The *MGMT* methylation status has been determined and reported previously [11, 32]. Expression of the *EGFRvIII* mutant, array comparative genomic hybridization (aCGH) data and gene expression data were available for a subgroup of patients [17, 21]. Additional *EGFR* amplification data were obtained by quantitative PCR as described [10]. Mutation analysis for *IDH1* and *IDH2* encompassing codon

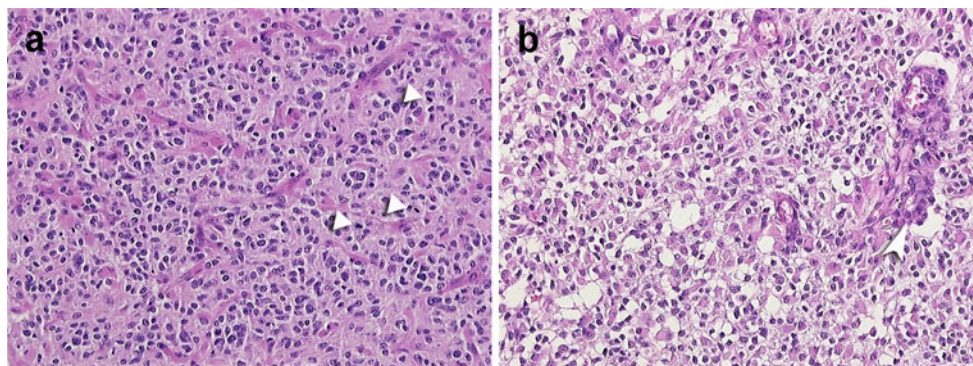


Fig. 1 Examples of histology in two tumors diagnosed as glioblastoma with oligodendroglioma-like component. **a** Area showing diffuse highly cellular and monotonous growth of tumor cells with a dense chromatin pattern, perinuclear halo formation and chicken-wire architecture of the microvasculature. **b** Highly cellular area showing rounded tumor cell nuclei with dense chromatin pattern and

perinuclear halo formation. See “Patients and methods” for the definitions used in the present study for recognition of oligodendroglioma-like component in glioblastoma. *Arrowheads* in **a** mitotic figures, *arrowhead* in **b** florid microvascular proliferation. **a**, **b** Hematoxylin and Eosin staining, original magnification $\times 200$

132 and 172, respectively, was performed by direct Sanger sequencing.

Statistics

The Fisher's exact test (for binary or nominal categorical data) and the Wilcoxon rank-sum test (for continuous or ordinal categorical data) were used in the comparisons of patient and disease characteristics between subgroups. Survival analyses were performed with Kaplan–Meier technique with log-rank statistics. The Cox regression was used for multivariate analyses. All Cox models were fit with age (≤ 50 , 51–60, >60), extent of surgery (total, partial, biopsy only), performance status (0, 1, 2), Mini Mental Score Examination (<27 , 27–30) and *MGMT* methylation status (unmethylated, methylated). Pathological features significant at a 5% level in univariate analyses were included in the multivariate model. A treatment effect was assessed using Peto's heterogeneity test (predictive value). No adjustment for multiple testing was performed in these exploratory analyses. SAS version 9.2 was used for statistical analyses.

Results

Histological diagnosis and subclassification

Central review comprised histological analysis of 360 of 573 patients enrolled (central review of Canadian patients was performed independently). Baseline characteristics have been published previously [32] and sub-cohort patient characteristics are summarized in Supplemental Table S1. Overall, the patient characteristics of this subset did not differ significantly from the overall study population, other than molecular markers that could be determined in patients who had undergone tumor resection in contrast to biopsy only. From the total of 360 cases reviewed, 6 were considered undiagnosable due to insufficient tissue or quality of the sections. Fifteen (4.2%) tumors did not fulfill the criteria for GBM and comprised 4 anaplastic astrocytomas (WHO

grade III; AA), 4 anaplastic oligoastrocytomas (WHO grade III, AOA), 1 anaplastic oligodendroglioma (WHO grade III; AO), 2 anaplastic ependymomas (WHO grade III), 2 pilocytic astrocytomas with malignant changes, 1 low grade glioma (WHO grade II) and 1 meningioma. Of the non-GBM tumors, 6 were in the RT and 9 in the RT/TMZ arm. The remaining 339 were diagnosed as GBM, of which 3 were subtyped as gliosarcoma and 6 as giant cell GBM. There was a 95% (338/354) consensus with regard to diagnosis of GBM versus non-GBM among the three neuropathologists. The median age of patients with confirmed GBM was 56 years of age (range 19–79) (Supplemental Table S2).

Frequency of GBM with an oligodendroglioma-like component

The criteria for GBM-O were met in 52 (15%) samples, at an expected frequency [12, 29, 37]. Subtyping of centrally confirmed GBM, including GBM-O, resulted in a 2:1 agreement for 24 cases, of which 16 overlapped with the debated cases for GBM versus non-GBM. In the group classified as GBM-O, two of five were considered as AOA and two as AO, by one of the neuropathologists. The median age of patients with GBM-O was lower than that of the other GBM patients (53 vs. 56 years, $p = 0.02$) (Supplemental Table S2).

GBM-O encompass a pathogenetically heterogeneous group

Evaluation of important prognostic molecular markers revealed the same frequency of *MGMT* methylation in GBM-O (47%, 16/34) versus the remaining GBM (46%, 60/131) (Table 1). Furthermore, combined loss of 1p/19q, a hallmark of oligodendroglial tumors and associated with better prognosis in anaplastic glioma [35], was a rare event, observed in a single GBM-O, confirmed by aCGH, and one GBM (Fig. 2; Table 1).

Next, we investigated if GBM-O exhibit a particular pathogenetic makeup. Mutations of the *IDH1* gene that are

Table 1 Tumor genetics of GBM-O versus GBM

	Overall cases in central review	Confirmed GBM (%)	GBM-O (%)	GBM (%)	<i>p</i> value ^a
Alterations					
meth <i>MGMT</i>		76/165 (46)	16/34 (47)	60/131 (46)	1.00
<i>IDH1</i> mut		9/130 (7)	6/32 (19)	3/98 (3)	0.007
Co-del 1p/19q		2/137 (1)	1/31 (3)	1/106 (1)	0.4
<i>EGFR</i> amp		70/131 (53)	22/31 (71)	48/100 (48)	0.038
<i>CDK4</i> amp		24/131 (18)	7/29 (24)	17/102 (17)	0.42
<i>MDM2</i> amp		13/131 (10)	4/30 (13)	9/101 (9)	0.49

Statistically significant values are given in bold

^a Fisher exact test

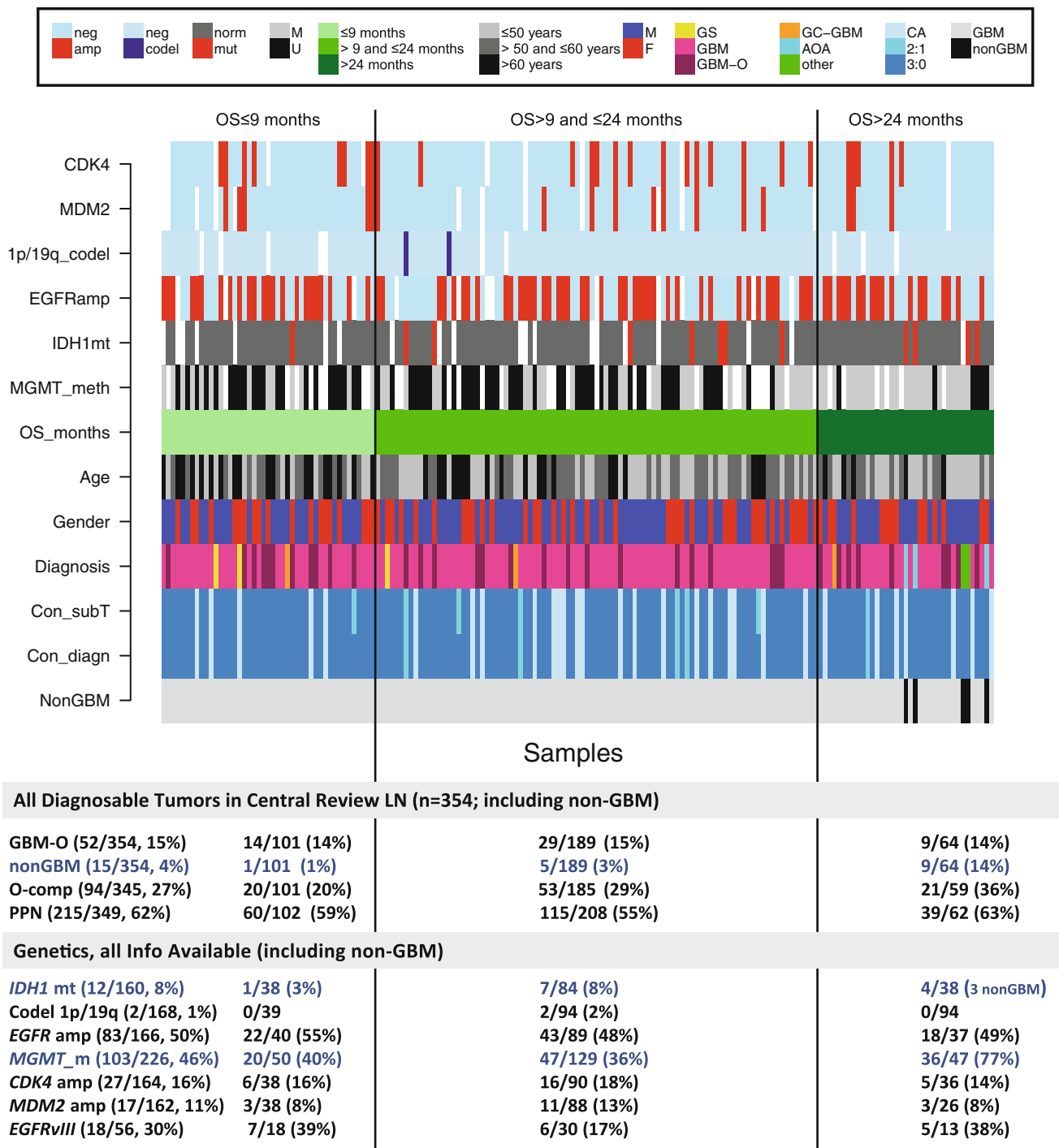


Fig. 2 Patterns of genetic alterations, diagnosis and outcome. Patient data for 175 cases with 3/6 genetic tests available were ordered according to overall survival (OS). Many features are rare, such as GBM subtypes, or genetic alterations like *IDH1* mutations. The visualization allows identification of patterns of genetic or clinical features that are enriched in either the short survival group or the long-term survival group. Gene amplification is represented in red (*CDK4*, *MDM2*, *EGFR*) and deletions in dark blue (co-deletion of 1p/19q). Mutation of *IDH1* is represented in red, *MGMT* methylated in gray and unmethylated in black. OS in months: light green short survival group (≤ 9 months); green intermediate survival group (> 9 and

< 24 months); dark green long-term survival group (≥ 24 months). Age < 50 years is represented in gray, 50–60 years in dark gray, and > 60 years in black. Red female, blue male. Pink diagnosis as GBM; purple GBM-O; yellow Gliosarcoma; orange giant cell GBM (GC-GBM); blue AOA; green other non-GBM diagnosis. Concordance of reviewers 3:0 for subtype (Con_subT) or diagnosis (Con_diagn) in dark blue; blue concordance 2:1; light blue diagnosis by Canadian central review. Diagnosis of non-GBM is indicated in black. White No information for all criteria. The associated table below shows the respective numbers. *EGFRvIII* information was available for only 56 cases and is not included in the upper panel

associated with better outcome in GBM [40] were significantly enriched in GBM-O (6/32, 19%) as compared to the remaining GBM (3/98, 3%; $p = 0.002$). Similarly, *EGFR* amplification that has been associated with older age and potentially worse outcome was present in 71% of GBM-O (22/31) and 48% of the remaining GBM (48/100) ($p = 0.03$). *IDH1* and *EGFR* alterations were mutually exclusive as reported before [40]. Intriguingly, of 31 GBM-O for which this genetic information was available, 6 carried the *IDH1R132H* mutation, 22 displayed an *EGFR* amplification, and only three had neither alteration. The presence of an *IDH1* or *IDH2* hot-spot mutation other than

IDH1R132H was excluded by direct sequencing in these three cases. The notion that the GBM-O phenotype identifies at least two pathogenetically distinct subgroups is further supported by classification according to the four gene expression-based subtypes proposed by Verhaak et al. [36]. Of 14 evaluable GBM-O, 5 grouped with the proneural, 6 with the classical, 2 with the mesenchymal and 1 with the neural GBM subtypes. In accordance with the reported mutation pattern of the four subgroups, all GBMs with an *IDH1* mutation were in the proneural group, while most *EGFR*-amplified and *EGFRvIII*-positive GBMs were in the classical subgroup (Fig. 3).

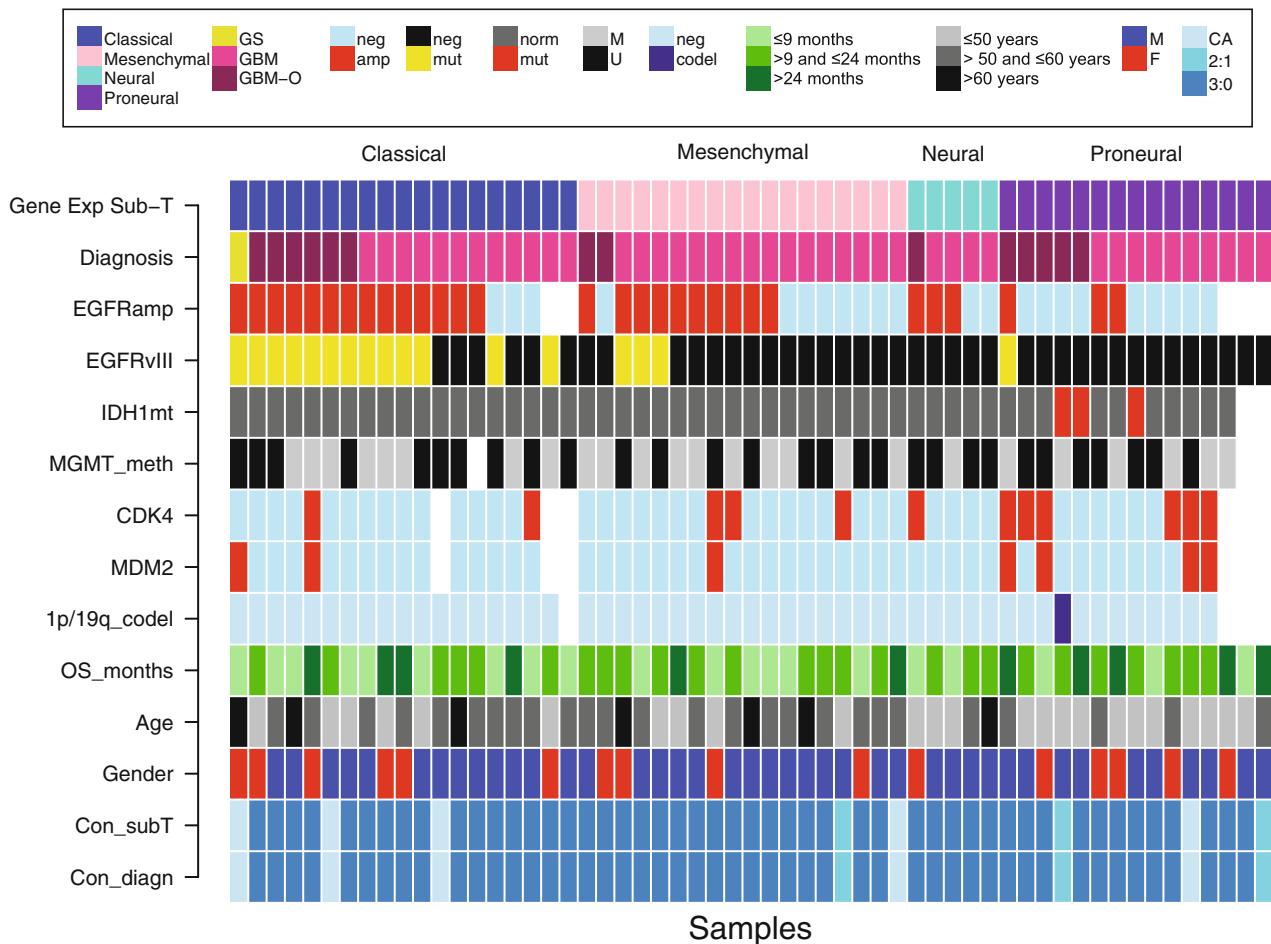


Fig. 3 Gene expression-based classification and GBM subtype. For 57 patients gene expression data, including for *EGFRvIII*, was available from frozen tumor tissue [21]. The tumor samples were classified according to the algorithm proposed by Verhaak et al. [36] into classic, mesenchymal, neural and proneural GBM. The samples are ordered by the gene expression-based classification, followed by diagnostic subtype, gliosarcoma (GS), GBM-O and GBM. The respective pathogenetic information and clinical information is the same as in Fig. 1. The enrichment of specific pathogenetic alterations, such as *IDH1* mutations in the proneural and *EGFR* amplification and *EGFRvIII* expression in the classical subtype, is in accordance with the report by Verhaak et al. [36]. Gene amplification is represented in

red (*CDK4*, *MDM2*, *EGFR*) and deletions in dark blue (co-deletion of 1p/19q). *EGFRvIII* expression determined by qRT-PCR is depicted in yellow. Mutation of *IDH1* is represented red, *MGMT* methylated in gray and unmethylated in black. OS in months: light green short survival group (≤ 9 months); green intermediate survival group (> 9 and < 24 months); dark green long-term survival group (≥ 24 months). Age < 50 is represented in gray, 50–60 in dark gray, and > 60 years in black. Red female, blue male. Pink diagnosis as GBM; purple GBM-O; yellow gliosarcoma (GS). Concordance of reviewers 3:0 for subtype (Con_subT) or diagnosis (Con_diagn) in dark blue; concordance 2:1 in blue; diagnosis by Canadian central review in light blue. White no information for all criteria

Survival of patients with GBM-O is not different from those with GBM

Patients with non-GBM pathology (15/354, 4%) were enriched in the patient group with overall survival (OS) exceeding 24 months (9/64, 14%), as compared to the short survival group (≤ 9 months, 1/101), and the intermediate group (5/189, 3%) ($p < 0.001$, Chi-square-test) (Fig. 1). Subsequently, only patients with confirmed GBM ($N = 339$) are included for further analysis of morphologic features and outcome. There was no difference in OS between GBM and GBM-O (logrank test, $p = 0.48$). Stratification by age (≤ 50 , 51–60 or >60) ($p = 0.55$) or *MGMT* methylation status ($p = 0.27$) did not differentiate survival in the two subgroups. When analyzing the GBM-O separately per randomized treatment arm, survival was not different for GBM-O in either arm (TMZ/RT \rightarrow TMZ arm, $p = 0.81$; RT-only arm, $p = 0.14$) (Fig. 4). The respective values for progression-free survival were similar ($p = 0.97$, TMZ/RT \rightarrow TMZ; $p = 0.2$, RT). Likewise, using less strict criteria, just the presence of any oligodendroglioma-like component did not show any association with outcome in either of the two treatment arms (Table 2). The apparent enrichment of patients with the presence of any oligodendroglioma-like component in the long survivor group as visualized in Fig. 2 was due to inclusion of patients where GBM was not confirmed.

Associations of histopathological features with tumor genetics

The MIB-1 labeling index was significantly higher in *MGMT* methylated GBM with a mean index of 38% ($N = 69$) as compared to 30% in *MGMT* unmethylated tumors ($N = 84$) ($p = 0.0015$). A trend for a higher MIB-1

labeling index was associated with *IDH1* mutations and *EGFR* amplifications ($p = 0.07$, $p = 0.09$). No significant association was observed between any morphologic feature and the *MGMT* methylation status.

Associations of tumor genetics and outcome

None of the genetic alterations investigated here was associated with a prognostic or a predictive value with the exception of *MGMT* methylation as previously reported (Supplementary Table S5) [32, 38]. Mutations of *IDH1* were rare in confirmed GBM (9/130; 7%, for which this information was available) as expected [25] and similarly distributed between the treatment arms (5, RT; 4, RT&TMZ), with five of eight assessable cases being *MGMT* methylated. These small numbers do not allow appropriate assessment of the prognostic value of *IDH1* mutations ($p = 0.7$, Supplementary Fig. S2). The patterns of genetic alterations and outcome are displayed in Fig. 2.

Presence of pseudopalisading necroses (PPN) is associated with a treatment effect of TMZ

Correlation of the distinct morphologic features assessed, such as type of necrosis, vascular pattern and cell differentiation, and including the MIB-1 (Ki67) labeling index (Supplementary Fig. S1), identified PPN as the only morphologic feature associated with outcome (Table 2). PPN was present in 63% of all GBM (212/339) and associated with a treatment effect (Fig. 5; Table 2). Addition of TMZ to RT was beneficial in the patient cohort exhibiting PPN ($p = 0.0002$), while no such effect was present in the absence of PPN ($p = 0.86$; Fig. 5a). Peto's interaction test was significant ($p = 0.026$; Fig. 5b) and borderline non-significant in a Cox interaction model adjusted for known

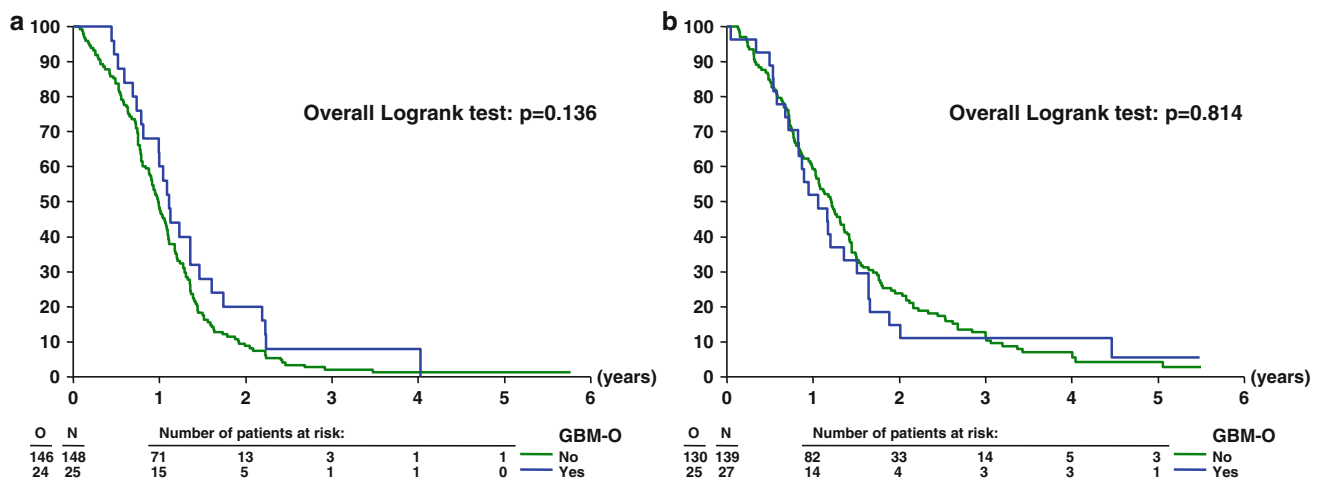


Fig. 4 GBM-O did not have better prognosis than all other GBMs. Kaplan–Meier curves show the OS of GBM versus GBM-O in the RT arm (log-rank test $p = 0.136$) (a) and the TMZ/RT \rightarrow TMZ arm ($p = 0.814$) (b)

Table 2 Morphologic features of confirmed GBM and OS ($N = 339$)

Subsample characteristics	Treatment			p value Fisher	Prognostic value for overall survival p value		
	RT ($N = 173$) N (%)	TMZ/RT ($N = 166$) N (%)	Total ($N = 339$) N (%)		Pooled	RT	TMZ/RT
Diagnosis							
Glioblastoma	145 (83.8)	133 (80.1)	278 (82.0)	0.69			
GBM-O	25 (14.5)	27 (16.3)	52 (15.3)				
Giant cell glioblastoma	2 (1.2)	4 (2.4)	6 (1.8)				
Gliosarcoma	1 (0.6)	2 (1.2)	3 (0.9)				
GBM confirmed							
GBM	148 (85.5)	139 (83.7)	287 (84.7)	0.65	0.48	0.14	0.81
GBM-O	25 (14.5)	27 (16.3)	52 (15.3)				
NECROSIS—large ischemic type							
No	34 (19.7)	23 (13.9)	57 (16.8)	0.19	0.79	0.18	0.20
Yes	139 (80.3)	143 (86.1)	282 (83.2)				
NECROSIS—pseudopalisading							
No	62 (35.8)	65 (39.2)	127 (37.5)	0.58	0.27	0.32	0.03
Yes	111 (64.2)	101 (60.8)	212 (62.5)				
NECROSIS—thrombosed vessels							
No	27 (15.6)	28 (16.9)	55 (16.2)	0.77	0.48	0.99	0.40
Yes	146 (84.4)	138 (83.1)	284 (83.8)				
Microvascular proliferation							
No	2 (1.2)	4 (2.4)	6 (1.8)	0.44	0.80	0.98	0.92
Yes	171 (98.8)	162 (97.6)	333 (98.2)				
Perivascular lymph							
No	133 (76.9)	128 (77.1)	261 (77.0)	0.90	0.89	0.39	0.40
Yes	38 (22.0)	35 (21.1)	73 (21.5)				
Missing	2 (1.2)	3 (1.8)	5 (1.5)				
Oligodendroglioma-like component							
No	129 (74.6)	120 (72.3)	249 (73.5)	0.80	0.24	0.29	0.52
Yes	44 (25.4)	44 (26.5)	88 (26.0)				
Missing	0 (0.0)	2 (1.2)	2 (0.6)				
Sarcomatous comp							
No	167 (96.5)	157 (94.6)	324 (95.6)	0.57	0.15	0.16	0.34
Yes	5 (2.9)	7 (4.2)	12 (3.5)				
Missing	1 (0.6)	2 (1.2)	3 (0.9)				
Multinucleated giant cells							
No	137 (79.2)	124 (74.7)	261 (77.0)	0.44	0.43	0.78	0.38
Yes	36 (20.8)	40 (24.1)	76 (22.4)				
Missing	0 (0.0)	2 (1.2)	2 (0.6)				
Gemistocytic cells							
No	124 (71.7)	123 (74.1)	247 (72.9)	0.54	0.41	0.70	0.65
Yes	49 (28.3)	41 (24.7)	90 (26.5)				
Missing	0 (0.0)	2 (1.2)	2 (0.6)				
Other prominent patterns							
No	157 (90.8)	141 (84.9)	298 (87.9)	0.21	0.82	0.13	0.75
Yes	14 (8.1)	20 (12.0)	34 (10.0)				
Missing	2 (1.2)	5 (3.0)	7 (2.1)				

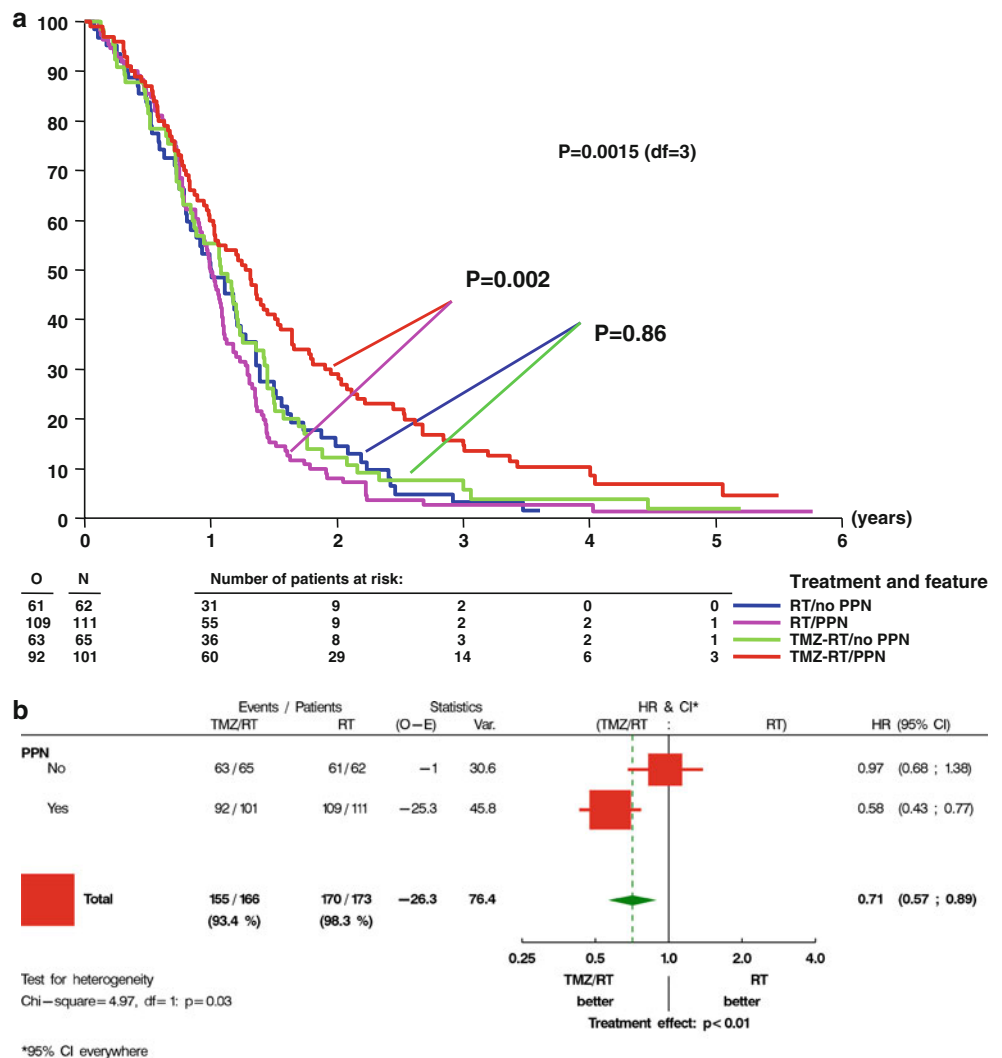
Table 2 continued

Subsample characteristics	Treatment			<i>p</i> value Fisher	Prognostic value for overall survival <i>p</i> value		
	RT (<i>N</i> = 173) <i>N</i> (%)	TMZ/RT (<i>N</i> = 166) <i>N</i> (%)	Total (<i>N</i> = 339) <i>N</i> (%)		Pooled	RT	TMZ/RT
MIB-1							
Median	30.0	30.0	30.0	0.08 ^a	0.13	0.65	0.24
Mean (SD)	32.72 (17.81)	36.40 (18.26)	34.53 (18.10)				
Range	5.0–80.0	5.0–90.0	5.0–90.0				
<i>N</i> obs	156	150	306				

Statistically significant values are given in bold

^a Wilcoxon rank-sum test

Fig. 5 The presence of pseudo-palisading necrosis is associated with a treatment effect. **a** The Kaplan–Meier curves visualize the overall outcome of the patients in the presence or absence of pseudo-palisading necrosis (PPN). In the presence of PPN, there is a treatment effect (RT vs. TMZ/RT $p = 0.002$), while in the absence of PPN, no such difference is observed (RT vs. TMZ/RT $p = 0.86$). **b** Forest Plot and Peto’s test of interaction between PPN and treatment for OS in all confirmed GBMs. Peto’s test was significant ($p = 0.03$) indicating that treatment effects differ significantly as a function of PPN



clinical prognostic factors ($p = 0.087$, Supplemental Table S3) not accounting for *MGMT* that was available only for a subset of 165 mostly resected tumors (Supplementary Table S1). This suggests that indeed PPN may identify a subgroup of chemo-sensitive GBM. The incidence of PPN was lower in patients with biopsy only (46 vs. 65.4%,

$p = 0.01$), while no association with age was observed ($p = 0.15$). To exclude a bias of potential underestimation of PPN in stereotactic biopsies resulting from the small sample size, and the fact that biopsy only by itself is an unfavorable prognostic factor, the analyses were repeated in patients who underwent a tumor resection. Peto’s test

was significant ($p = 0.040$, Supplementary Fig. S3) and the adjusted Cox interaction model including *MGMT* was borderline nonsignificant ($p = 0.063$, Supplementary Table S4). A similar treatment effect of PPN was observed for PFS ($p < 0.0001$) in the TMZ arm, while there was a trend in the RT arm ($p = 0.078$).

Discussion

The present study was performed to assess prognostic significance of morphological features of GBM in the registration trial for temozolomide, with a focus on GBM-O. Classification of GBM was in high concordance (>95%) between the 59 centers and central review. Expectedly, reclassification as a non-GBM histology was significantly enriched among long-term survivors (Fig. 2). The trial analyses and respective reports were on an intention-to-treat basis [32], and hence include patients with non-GBM histology.

Identification of unambiguous morphologic features with a prognostic or predictive value within GBM would be clinically valuable, as such markers could be easily implemented in routine histopathologic diagnostics. The recognized phenotypical GBM variants, giant cell GBM and gliosarcoma are rare (6, <2% and 3, <1% in this study) [15], precluding reliable assessment of a potential prognostic significance when patients are treated with the current standard of care. Evaluation of the prognostic value of an oligodendroglioma-like component in an otherwise classic GBM revealed no association with a more favorable disease course in either of the two treatment arms, in contrast to previous studies on GBM-O [9, 12, 16, 18, 29]. This discrepancy might be explained by the fact that most studies were performed in the pre-TMZ chemotherapy era. GBM-O, as defined in this report, seems to benefit similarly from chemoradiotherapy, in line with the identical *MGMT* methylation frequency compared to other GBMs that differ from frequencies reported for AO and AOA of over 70% [5, 20, 27, 39]. Further, the delineation of “pure” GBM versus GBM-O, and AOA and AO is difficult, as reflected in variable frequencies of reported 1p/19q co-deletions in these studies ranging from 0 to over 20% for the GBM-O subgroup [9, 12, 13, 16, 18, 29].

This study uncovered that GBM-O encompasses at least two distinct pathogenetic subgroups, characterized either by *EGFR* amplifications or *IDH1* mutations, and further supported by respective expression-based classification (Fig. 3). GBM-O, as defined here, may in part overlap with the small cell variant of GBM with high cellularity, diffuse more or less monotonous growth and relatively small, partly rounded nuclei that is known for increased *EGFR* amplification frequencies [12, 18]. Conversely, GBM with

IDH mutations are now recognized as a distinct subtype with a different pathogenetic/epigenetic origin, evolving from lower grade glioma with high frequencies of *IDH* mutations, characteristic of secondary GBM [1, 23, 40]. Interestingly, *IDH* mutant gliomas are associated with a DNA hypermethylation phenotype [24]. This association has recently also been reported in leukemia, identifying a new prognostic subtype, and mechanistically linking aberrant metabolism (onco-metabolite) with epigenetic deregulation [6, 26]. Our finding that recognition of an oligodendroglioma-like phenotype in otherwise classic GBM associates two completely different genetic/epigenetic GBM subtypes is a surprise and questions the clinical utility of morphologic identification of GBM-O. The introduction in the 2007 WHO classification of high-grade malignant oligoastrocytic tumors with necrosis as GBM-O [14] has led to substantial controversy among pathologists [30] and will certainly have to be re-visited given the recently discovered distinct pathogenetic/epigenetic evolution. Determination of oncogenetic events such as *IDH* status and 1p/19q co-deletions provide a more promising tool for robust and reproducible (sub) classification of malignant gliomas [8].

Evaluation of distinct morphologic features in this homogeneously treated patient population identified PPN as potentially associated with benefit from combined chemoradiotherapy. Presence of PPN may reflect the tumor milieu including the tumor vascularization type, which may have an effect on drug perfusion and thereby on response to chemotherapy. Pseudopalisades are enriched for hypoxic and apoptotic tumor cells, with a lower relative proliferation index, and are frequently associated with a central degenerating or thrombosed vascular lumen [2, 28]. Tumor-associated vascular injury has been associated with factors released from glioma cells after genetic alterations such as *EGFR* amplifications or cellular stress conditions such as hypoxia [3, 28]. Based on a comprehensive analysis of PPN in human GBM and experimental models, it has been hypothesized that pseudopalisades comprise hypoxic tumor cells migrating away from dysfunctional vessels [2, 28]. However, the presence of PPN does not directly correlate with hypoxia as suggested by gene expression profiles available for 50 patients of this cohort [21, 22]. No correlation was observed with the previously identified hypoxia-induced gene expression signature, while the *EGFR* expression signature (G25) was significantly associated with the presence of PPN ($p = 0.02$). Evaluation of associations of PPN with previously identified expression signatures in appropriately powered studies may indicate underlying molecular mechanisms that merit further analysis for improvement of therapy. The respective hypotheses may be tested in the database of ‘The Cancer Genome Atlas’ (TCGA) once the morphologic information

is publicly available [36]. In contrast to our study, Homma et al. [12] reported an association of the presence of any type of necrosis with worse outcome. This discrepancy may be explained by the fact that all these patients were treated before the TMZ era (before 1994) and likely received RT alone.

This study has shown that systematic combined morphologic and molecular characterization of tumor samples of patients enrolled in clinical trials is instrumental for validating and identifying new prognostic and predictive factors that will have an impact on clinical practice. This was an exploratory study requiring validation in an independent data set of a homogenous patient population treated with combined chemo-radiotherapy. The limited numbers of samples available for molecular analyses unfortunately reduced the power of the study, once more emphasizing the importance of collecting sufficient tissues for all patients enrolled in clinical trials.

Acknowledgments We thank all the patients who participated in the study and provided informed consent for translational research on their tumor tissues. We acknowledge the great contributions of the local pathologists, and the physicians and nurses taking care of the patients. We thank Solange Gros and Sylviane Trepey for their excellent technical support. Translational research in this study was supported by the Swiss National Science Foundation 3100A0_122557/1 (MEH), the Amadéo and Nélia Barletta Foundation (MEH, RS), the Jacqueline Seroussi Foundation (MEH) and the EORTC (TRF/04/01, TRF/02/03). Additional support was given by grants from the National Cancer Institute (5U10 CA11488-30 through 2U10 CA011488-41; Bethesda, Maryland, USA) and by the EORTC Charitable Trust. The content of this manuscript is solely the responsibility of the authors and does not necessarily reflect the official views of the National Cancer Institute.

Conflict of interest MEH is an advisor to MDxHealth. MEH, MW, MJvdB, ROM and RS have an advisory role and have received honoraria from MSD. CH and AvD have a licensing agreement with Dianova GmbH.

References

- Balss J, Meyer J, Mueller W et al (2008) Analysis of the IDH1 codon 132 mutation in brain tumors. *Acta Neuropathol* 116:597–602
- Brat DJ, Castellano-Sanchez AA, Hunter SB et al (2004) Pseudopalisades in glioblastoma are hypoxic, express extracellular matrix proteases, and are formed by an actively migrating cell population. *Cancer Res* 64:920–927
- Brat DJ, Van Meir EG (2004) Vaso-occlusive and prothrombotic mechanisms associated with tumor hypoxia, necrosis, and accelerated growth in glioblastoma. *Lab Invest* 84:397–405
- Capper D, Weissert S, Balss J et al (2009) Characterization of R132H mutation-specific IDH1 antibody binding in brain tumors. *Brain Pathol* 20:245–254
- Dong SM, Pang JC, Poon WS et al (2001) Concurrent hypermethylation of multiple genes is associated with grade of oligodendroglial tumors. *J Neuropathol Exp Neurol* 60:808–816
- Figuerola ME, Abdel-Wahab O, Lu C et al (2010) Leukemic IDH1 and IDH2 mutations result in a hypermethylation phenotype, disrupt TET2 function, and impair hematopoietic differentiation. *Cancer Cell* 18:553–567
- Gorlia T, van den Bent MJ, Hegi ME et al (2008) Nomograms for predicting survival of patients with newly diagnosed glioblastoma: prognostic factor analysis of EORTC and NCIC trial 26981-22981/CE.3. *Lancet Oncol* 9:29–38
- Hartmann C, Hentschel B, Wick W et al (2010) Patients with IDH1 wild type anaplastic astrocytomas exhibit worse prognosis than IDH1-mutated glioblastomas, and IDH1 mutation status accounts for the unfavorable prognostic effect of higher age: implications for classification of gliomas. *Acta Neuropathol* 120:707–718
- He J, Mokhtari K, Sanson M et al (2001) Glioblastomas with an oligodendroglial component: a pathological and molecular study. *J Neuropathol Exp Neurol* 60:863–871
- Hegi ME, Diserens A-C, Bady P et al (2011) Pathway analysis of glioblastoma tissue after preoperative treatment with the EGFR tyrosine kinase inhibitor gefitinib—a phase II trial. *Mol Cancer Ther* 11:102–112
- Hegi ME, Diserens AC, Gorlia T et al (2005) MGMT gene silencing and benefit from temozolomide in glioblastoma. *N Engl J Med* 352:997–1003
- Homma T, Fukushima T, Vaccarella S et al (2006) Correlation among pathology, genotype, and patient outcomes in glioblastoma. *J Neuropathol Exp Neurol* 65:846–854
- Ichimura K, Pearson DM, Kocalkowski S et al (2009) IDH1 mutations are present in the majority of common adult gliomas but rare in primary glioblastomas. *Neuro Oncol* 11:341–347
- Kleihues P, Burger PC, Aldape KD et al (2007) Glioblastoma. In: Louis DN, Ohgaki H, Wiestler OD, Cavenee WK (eds) WHO classification of tumours of the central nervous system. International Agency for Research on Cancer (IARC), Lyon, pp 33–46
- Kleihues P, Cavenee WK (2000) Pathology and genetics of tumours of the nervous system. IARC Press, Lyon
- Kraus JA, Lamszus K, Glesmann N et al (2001) Molecular genetic alterations in glioblastomas with oligodendroglial component. *Acta Neuropathol* 101:311–320
- Lambiv WL, Vassallo I, Delorenzi M et al (2011) The Wnt inhibitory factor 1 (WIF1) is targeted in glioblastoma and has a tumor suppressing function potentially by induction of senescence. *Neuro Oncol* 13:736–747
- Miller CR, Dunham CP, Scheithauer BW et al (2006) Significance of necrosis in grading of oligodendroglial neoplasms: a clinicopathologic and genetic study of newly diagnosed high-grade gliomas. *J Clin Oncol* 24:5419–5426
- Mirimanoff RO, Gorlia T, Mason W et al (2006) Radiotherapy and temozolomide for newly diagnosed glioblastoma: recursive partitioning analysis of the EORTC 26981/22981-NCIC CE3 phase III randomized trial. *J Clin Oncol* 24:2563–2569
- Mölleremann M, Wolter M, Felsberg J et al (2005) Frequent promoter hypermethylation and low expression of the MGMT gene in oligodendroglial tumors. *Int J Cancer* 113:379–385
- Murat A, Migliavacca E, Gorlia T et al (2008) Stem cell-related “self-renewal” signature and high epidermal growth factor receptor expression associated with resistance to concomitant chemoradiotherapy in glioblastoma. *J Clin Oncol* 26:3015–3024
- Murat A, Migliavacca E, Hussain SF et al (2009) Modulation of angiogenic and inflammatory response in glioblastoma by hypoxia. *PLoS ONE* 4:e5947
- Nobusawa S, Watanabe T, Kleihues P et al (2009) IDH1 mutations as molecular signature and predictive factor of secondary glioblastomas. *Clin Cancer Res* 15:6002–6007

24. Noushmehr H, Weisenberger DJ, Diefes K et al (2010) Identification of a CpG island methylator phenotype that defines a distinct subgroup of glioma. *Cancer Cell* 17:419–420
25. Ohgaki H, Kleihues P (2011) Genetic profile of astrocytic and oligodendroglial gliomas. *Brain Tumor Pathol* 28:177–183
26. Prensner JR, Chinnaiyan AM (2011) Metabolism unhinged: IDH mutations in cancer. *Nat Med* 17:291–293
27. Riemenschneider MJ, Hegi ME, Reifenberger G (2010) MGMT promoter methylation in malignant gliomas. *Target Oncol* 5:161–165
28. Rong Y, Durden DL, Van Meir EG et al (2006) ‘Pseudopalisading’ necrosis in glioblastoma: a familiar morphologic feature that links vascular pathology, hypoxia, and angiogenesis. *J Neuropathol Exp Neurol* 65:529–539
29. Salvati M, Formichella AI, D’Elia A et al (2009) Cerebral glioblastoma with oligodendroglial component: analysis of 36 cases. *J Neurooncol* 94:129–134
30. Scheithauer BW, Fuller GN, VandenBerg SR (2008) The 2007 WHO classification of tumors of the nervous system: controversies in surgical neuropathology. *Brain Pathol* 18:307–316
31. Seiz M, Tuettenberg J, Meyer J et al (2010) Detection of IDH1 mutations in gliomatosis cerebri, but only in tumors with additional solid component: evidence for molecular subtypes. *Acta Neuropathol* 120:261–267
32. Stupp R, Hegi ME, Mason WP et al (2009) Effects of radiotherapy with concomitant and adjuvant temozolomide versus radiotherapy alone on survival in glioblastoma in a randomised phase III study: 5-year analysis of the EORTC-NCIC trial. *Lancet Oncol* 10:459–466
33. Stupp R, Mason WP, van den Bent MJ et al (2005) Radiotherapy plus concomitant and adjuvant temozolomide for glioblastoma. *N Engl J Med* 352:987–996
34. van den Bent MJ, Brandes AA, Rampling R et al (2009) Randomized phase II trial of erlotinib versus temozolomide or carmustine in recurrent glioblastoma: EORTC Brain Tumor Group Study 26034. *J Clin Oncol* 27:1268–1274
35. van den Bent MJ, Carpentier AF, Brandes AA et al (2006) Adjuvant procarbazine, lomustine, and vincristine improves progression-free survival but not overall survival in newly diagnosed anaplastic oligodendrogliomas and oligoastrocytomas: a randomized European Organisation for Research and Treatment of Cancer phase III trial. *J Clin Oncol* 24:2715–2722
36. Verhaak RG, Hoadley KA, Purdom E et al (2010) Integrated genomic analysis identifies clinically relevant subtypes of glioblastoma characterized by abnormalities in PDGFRA, IDH1, EGFR, and NF1. *Cancer Cell* 17:98–110
37. Vordermark D, Ruprecht K, Rieckmann P et al (2006) Glioblastoma multiforme with oligodendroglial component (GBMO): favorable outcome after post-operative radiotherapy and chemotherapy with nimustine (ACNU) and teniposide (VM26). *BMC Cancer* 6:247
38. Weller M, Felsberg J, Hartmann C et al (2009) Molecular predictors of progression-free and overall survival in patients with newly diagnosed glioblastoma: a prospective translational study of the German Glioma Network. *J Clin Oncol* 27:5743–5750
39. Wick W, Hartmann C, Engel C et al (2009) NOA-04 randomized phase III trial of sequential radiochemotherapy of anaplastic glioma with procarbazine, lomustine, and vincristine or temozolomide. *J Clin Oncol* 27:5874–5880
40. Yan H, Parsons DW, Jin G et al (2009) IDH1 and IDH2 mutations in gliomas. *N Engl J Med* 360:765–773